7. Rowe CC, Berkovic SF, Sia STB, et al. Localization of epileptic foci with postictal SPECT. *Ann Neurol* 1989;26:660.
8. Lee BI, Markland ON, Wellman HN, et al. HIPDM-SPECT in patients with medically intractable complex partial seizures, ictal study. *Arch Neurol* 1988;45:397–402.
9. Shen W, Lee BI, Park HM, et al. HIPDM-SPECT brain imaging in the presurgical evaluation of patients with intractable seizures. *J Nucl Med* 1990;31:1280–1284.
10. Baron JC, Bousser MG, Comar D, Castaigne P. Crossed cerebellar diaschisis in human supratentorial infartion [Abstract]. *Ann Neurol* 1980;8:128.
11. Park CH, Kim SM, Streletz LJ, Zhang J, Intenzo C. Reverse crossed cerebellar diaschisis in partial complex seizures related to herpes simplex encephalitis. *Clin Nucl Med* 1992;17:732–735.
12. Duncan R, Patterson J, Bone I, Wyper DJ. Reversible cerebellar diaschisis in focal epilepsy. *Lancet* 1987;2:625–626.
13. Piero VD, Chollet F, Dolan RJ, Thomas DJ, Frackowiak R. The functional nature of cerebellar diaschisis. *Stroke* 1990;21:1365–1369.
14. Kurthen M, Reichmann K, Linke DB, et al. Crossed cerebellar diaschisis in intracarotid sodium amytal procedures: a SPECT study. *Acta Neurol Scand* 1990;81: 416–422.

Heterogeneity of Cerebral Hemodynamics and Metabolism in Carotid Artery Disease

David B. Duncan, Gereon R. Fink, Martin Wirth, Jan Löttgen, Gunter Pawlik and Wolf-Dieter Heiss
Max-Planck-Institut for Neurology, Köln, Germany and University Clinic for Neurology, Köln, Germany

Methods: Eight patients with severe unilateral carotid stenosis (>70%) were evaluated using PET to assess parametric changes in cerebral blood flow, blood volume, metabolic rate for oxygen, metabolic rate for glucose, oxygen extraction fraction and glucose extraction fraction. We performed these examinations because clinical history and physical exam results suggested possible cerebral vascular disease. Four patients were neurologically asymptomatic with other signs of peripheral vascular disease (e.g., episodic vertigo, TIA and claudication). All patients had normal neurologic examinations and normal CT or MRI studies. PET images were analyzed by two methods. First, regions of interest were used for the entire hemisphere, vascular territories and borderzones. Regions ipsilateral to the carotid stenosis were compared to respective regions in the contralateral hemisphere using Student's t-test. Second, visual inspection of each image was performed. **Results:** Statistical analysis demonstrated no significant differences between hemodynamic and metabolic parameters for regions ipsilateral to the carotid stenosis and contralateral homotopic reference regions. Upon visual examination, however, all patients had focal changes in either cerebral blood flow, blood volume, glucose extraction fraction and/or oxygen extraction fraction. **Conclusion:** Visual inspection is important in the evaluation of pathophysiological changes caused by unilateral carotid stenosis. Clinical decisions in patients with carotid artery disease should be based on careful visual examinations and statistical analyses of appropriately selected regions.

Key Words: carotid artery disease; metabolism; cerebral blood flow; PET

J Nucl Med 1996; 37:429–432

PET imaging of the brain continues to play an important role in the assessment of cerebrovascular disease. One of PET's many clinical uses is the evaluation of hemodynamically significant carotid artery disease for evidence of impaired cerebral blood circulation. This is a relatively crucial issue, since researchers hope to prevent the occurrence of a cerebrovascular accident and possible life-long disability by medical treatment or carotid endarterectomy.

A primary concern in this particular patient population is initial presentation. The results of investigations which examine the frequency of strokes as the first manifestation of hemodynamically significant carotid artery disease have been variable. Investigators report occurrence rates of stroke ranging from 0.6% to 19.1% in these patients (*1–3*). In clinical practice, it is generally believed that patients with hemodynamically significant carotid artery disease have an approximately 20%–30% chance of developing symptoms which by and large will be transient. There remains, however, a significant proportion of these patients who will probably present initially as a stroke without warning (*4*). Exploration of the hemodynamic status thus needs to be made as early as possible during the course of the disease. Since hemodynamic reserve and the effect of decreasing perfusion on tissue oxygen metabolism (*5*) can be assessed with PET, it has been used in an attempt to detect patients at risk. Several investigators, using the results of statistical region of interest (ROI) analysis, felt that the degree of carotid stenosis correlates poorly with the hemodynamic status of the ipsilateral cerebral circulation (*6–11*). Others claimed to have found a significant reduction of cerebral blood flow and hemodynamic reserve capacity in the borderzone regions between the anterior cerebral artery (ACA) and middle cerebral artery (MCA) ipsilateral to the carotid stenosis (*12,13*).

We present a PET study of eight patients with hemodynamically significant (>70%) unilateral carotid stenosis in whom the cerebral hemodynamic and metabolic status was evaluated. The following parameters were measured: cerebral metabolic rate for glucose (CMRgl), cerebral metabolic rate for oxygen ($CMRO_2$), oxygen extraction fraction (OEF), glucose extraction fraction (GEF), mean vascular transit time (MVTT), cerebral blood volume (CBV), cerebral blood flow (CBF) and cerebral metabolic ratio (CMR).

METHODS

Eight patients (5 men, 3 women; aged 56–70 yr, mean 64.5 ± 2.0 yr) with 70% or greater unilateral internal carotid artery stenosis were studied. Informed consent was obtained from all patients. Patients were referred for neurological assessment and Doppler sonography because of suspected cerebral vascular disease due to: (a) other signs of peripheral vascular disease (e.g., intermittent claudication, etc., n = 4), (b) episodic vertigo (n = 2), (c) transient ischemic attack (TIA) with mildly slurred speech (n = 1) and (d) nonspecific symptoms consisting of bilateral hand and foot paresthesias (n = 1). All patients had normal neurologic examinations and normal CT or MRI studies. The grade of stenosis was determined in all patients using carotid Doppler sonography. The study criterion was >70% unilateral carotid stenosis. Two patients had 70% stenosis, three patients had 80% stenosis and three patients had 90% stenosis.

Received Jan. 19, 1995; revision accepted Jul. 30, 1995.
For correspondence or reprints contact: D.B. Duncan, MD, Hospital for Joint Diseases, Room 1615, 301 East 17th St., New York, NY 10003.

TABLE 1
Metabolic and Hemodynamic Data for Borderzones and Vascular Territories Ipsilateral and Contralateral (Control) to Hemodynamically Significant Carotid Stenosis

Measurement	ACA-MCA zone		MCA-PCA zone	
	IPSI	Control	IPSI	Control
CBF (ml/100 g/min)	40.2 ± 9.26	41.8 ± 8.94	38.3 ± 7.81	40.6 ± 9.14
CBV (ml/100 g)	2.6 ± 0.54	2.4 ± 0.45	3.3 ± 1.28	3.1 ± 0.89
MVTT (sec)	4.1 ± 1.45	3.6 ± 1.10	5.0 ± 1.66	4.7 ± 1.30
CMRO2 (μmole/100 g/min)	183.3 ± 31.51	190.0 ± 25.01	177.0 ± 19.98	187.8 ± 25.43
OEF (%)	51.4 ± 12.27	52.0 ± 13.08	48.2 ± 19.93	51.9 ± 12.50
CMRgl (μmole/100 g/min)	30.7 ± 4.43	31.1 ± 4.80	27.4 ± 3.34	28.2 ± 4.12
GEF (%)	15.1 ± 5.11	14.6 ± 4.55	14.1 ± 4.83	13.7 ± 4.48
CMR (%)	16.7 ± 4.22	16.4 ± 3.93	15.5 ± 5.41	15.0 ± 3.52

Measurement	ACA		MCA		PCA	
	IPSI	Control	IPSI	Control	IPSI	Control
CBF (ml/100 g/min)	40.8 ± 8.93	43.0 ± 8.71	41.7 ± 9.50	44.1 ± 9.98	41.1 ± 8.42	43.7 ± 10.25
CBV (ml/100 g)	3.0 ± 0.68	2.9 ± 0.35	3.3 ± 0.67	3.1 ± 0.34	3.8 ± 0.84	3.7 ± 0.77
MVTT (sec)	4.6 ± 1.38	4.2 ± 0.91	5.0 ± 1.19	4.4 ± 0.89	5.7 ± 1.20	5.0 ± 1.46
CMRO2 (μmole/100 g/min)	183.9 ± 28.14	190.3 ± 31.27	192.4 ± 26.15	194.7 ± 28.02	187.3 ± 18.49	187.0 ± 17.90
OEF (%)	51.6 ± 12.37	49.6 ± 11.70	53.3 ± 13.52	50.0 ± 12.47	49.4 ± 12.31	48.1 ± 10.80
CMRgl (μmole/100 g/min)	30.3 ± 4.28	30.6 ± 4.65	30.0 ± 4.93	30.0 ± 4.50	27.4 ± 3.62	28.2 ± 4.07
GEF (%)	14.7 ± 4.88	14.0 ± 4.57	14.2 ± 4.75	13.4 ± 4.29	13.1 ± 4.24	12.7 ± 3.88
CMR (%)	16.5 ± 3.93	16.1 ± 3.98	15.6 ± 3.94	15.4 ± 3.80	14.6 ± 3.93	15.1 ± 2.99

Values are mean ± s.d. (n = 8).

ACA = anterior cerebral artery; MCA = middle cerebral artery; PCA = posterior cerebral artery; ACA-MCA zone = anterior border zone; MCA-PCA ZONE = posterior border zone; CBF = cerebral blood flow; CBV = cerebral blood volume; MVTT = mean vascular transit time; $CMRO_2$ = cerebral metabolic rate of oxygen; OEF = oxygen extraction fraction; CMRGL = cerebral metabolic rate of glucose; GEF = glucose extraction fraction; CMR = cerebral metabolic ratio.

All PET studies were performed consecutively on a four-ring PET camera with an in-plane resolution of 7.8 mm (FWHM) that permited simultaneous scanning of seven transaxial 11-mm thick slices. The patients were examined in the resting state with eyes closed and ears unplugged in a room with dimmed lights and low ambient noise. Positioning was achieved with a two-dimensional laser beam facility. All patients were scrutinized for any changes in head movement.

Regional CBF was measured dynamically over 300 sec (*14*) after intravenous injection of 40 mCi ^{15}O-labeled water (*15*). For each pixel, blood flow and partition coefficients (lambda) were determined. For measurements of $CMRO_2$ and OEF, in accordance with the single breath technique, the patient inhaled 100 mCi of $^{15}O_2$ in room air and data were accumulated over 180 sec. Using the operational equation of Mintun et al. (*16*), OEF and $CMRO_2$ were computed on a pixel-by-pixel basis. CBV and MVTT were measured according to the method described by Grubb et al. (*17*) using a closed inhalation system filled with 100 mCi ^{15}O-labeled carbon monoxide. CBV was calculated for each pixel. Images of MVTT were calculated pixel-by-pixel as the ratio of CBV to CBF. For the determination of CMRgl and GEF, the patients were injected intravenously with 5 mCi ^{18}F-labeled 2-fluoro-2-deoxy-D-glucose (FDG) (*18*). All oxygen studies comprised seven slices, while in CMRgl studies another set of seven intercalated slices were recorded to allow for three-dimensional image reconstruction. The CMRgl was calculated pixel-by-pixel using a K_1, k_2, k_3 optimization procedure and a fixed value of 0.42 (*19*) for the lumped constant. The GEF images were calculated pixel-by-pixel using the respective values of CMRgl, CBF and plasma glucose concentration. CMR images reflecting metabolic imbalance (e.g., anaerobic glycolysis) were calculated pixel-by-pixel as the CMRgl-to-$CMRO_2$ ratio. The investigative and scanning procedures have been described in detail elsewhere (*20,21*).

If there were any head movements between the ^{15}O sequence (CBF, $CMRO_2$ and CBV) and the CMRgl measurement, numerical realignment of the CMRgl images with respect to the CBF images was performed by a three-dimensional alignment procedure (*22*).

Each tomographic image was initially scrutinized for any focal or regional changes in measured parameters visually. Then, ROIs were placed using a semiautomatic procedure based on an adjustable map (*23*) with respect to cortical vascular territories and major brain structures. The entire set of seven slices was mapped using these standard geometrical ROIs. Based on descriptions by Damasio (*24*) and van der Eecken and Adams (*25*), the ROIs were then grouped into clusters representing an entire hemisphere, vascular territories [ACA, MCA and posterior cerebral artery (PCA)] or borderzones (ACA-MCA zone and MCA-PCA zone) ipsilateral and contralateral to the carotid stenosis. Metabolic and hemodynamic parameters for each cluster were calculated as the average of all regions, weighted by region size.

Descriptive statistics are presented as the arithmetic mean ± s.d. Cluster regions ipsilateral to the carotid stenosis were compared with the values obtained from the contralateral homotopic reference regions using a Student's t-test. Statistical calculations were performed using commercial software (SAS Institute, Inc., Cary, NC).

RESULTS

Quantitative evaluation of entire hemispheres revealed decreased mean values for CBF as well as increased values for MVTT, CBV and OEF ipsilateral to the carotid stenosis. Similar changes were also observed in the vascular territories (Table 1). The mean values for borderzone regions demonstrated decreased CBF (MCA-PCA greater than ACA-MCA) plus increases in CBV and MVTT. No increases in OEF,

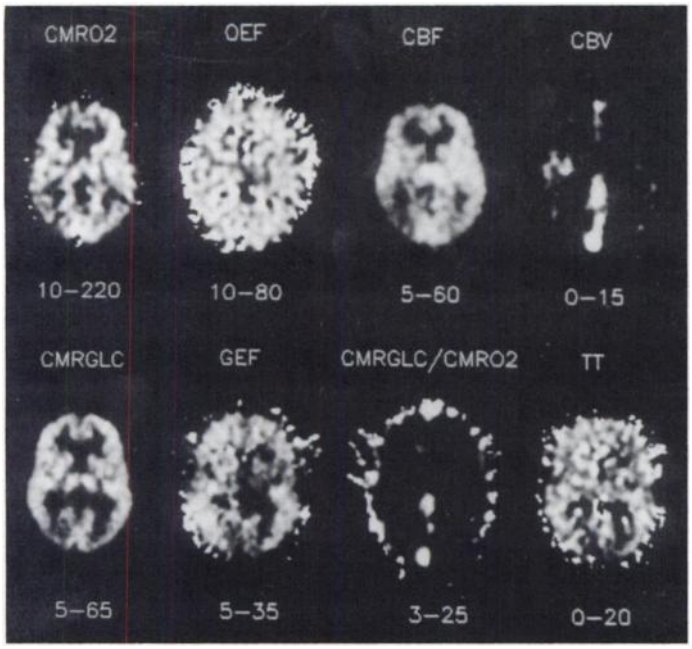

FIGURE 1. PET study in a patient with 90% right-sided unilateral carotid stenosis shows ipsilateral right-sided (viewers left) decreased CBF, increased CBV, increased GEF, increased OEF but normal $CMRO_2$ and CMRgl.

however, were observed (Table 1). Upon statistical analysis, there were no significant differences for any of the parameters tested between regions (entire hemisphere, vascular territories and borderzones) ipsilateral and contralateral to the carotid stenosis.

Upon visual examination, all patients showed focal changes within the MCA territory ipsilateral to the carotid stenosis in at least one or more of the hemodynamic or metabolic parameters measured. Three patients showed CBF reductions, two patients had decreased CBF with compensatory vasodilatation (increased CBV), two patients demonstrated decreased CBF with corresponding increases in the OEF and one patient had widespread changes in the distribution of both the ACA and MCA consisting of decreased CBF with compensatory vasodilatation, as well as increases in both GEF and OEF (Fig. 1). No patient showed that any visually identifiable changes could be localized to those areas representing the anterior and posterior borderzones.

DISCUSSION

Diagnosis and Assessment of Carotid Artery Disease

Previously, the degree of ipsilateral carotid stenosis was used to estimate cerebral hemodynamic status. Based on earlier studies, it has been argued that critical reductions in blood flow occurred when arteriographic analysis revealed up to 50%–75% occlusion of the vessel (*26,27*). Other studies, however, suggest that in estimating perfusion one should not rely just on the degree of stenosis, since collateral circulation also appears to play a significant role (*28*). Both stenosis and collateral circulation can be efficiently visualized using arteriography or duplex or transcranial Doppler technology; none of these techniques, however, are capable of evaluating CBF with respect to cerebral metabolic demands (*29*).

PET in Carotid Artery Disease

With PET, changes of metabolic (OEF, $CMRO_2$, GER, CMRgl) and hemodynamic (CBV, CBF) parameters are used to classify three stages of increasing hemodynamic compromise (*10*). Several studies have used this methodology to evaluate the hemodynamic status of the cerebral hemisphere ipsilateral to a significant carotid artery stenosis. These results, however, have been extremely controversial. When looking at arterial territories alone, it has been demonstrated using ROI analysis techniques that ipsilateral changes in hemodynamic status do not correlate with the degree of stenosis (*6–10*). Other investigators used similar methods to look at borderzone regions between areas of major cerebral artery blood supply and found contrasting results. LeBlanc et al. (*12,13*) found clear signs of hemodynamic compromise in the ipsilateral anterior border zone, while another investigator reported no evidence of significant change in these areas (*11*).

Technical Considerations

Statistical evaluation of PET images of patients with chronic cerebrovascular disease can obviously cause several problems that could lead to misinterpretation of the data. Errors due to image noise and artifacts are easily recognized, but unfortunately pixel-by-pixel analysis is extremely sensitive to such noise and artifacts. Any attempt to perform pixel-by-pixel analysis would require heavy smoothing and filtering which would result in a decrease in the effective resolution of up to 15–20 mm FWHM (*30*). ROI placement can also be a major source of variance. If a small ROI is used, then data can possibly be biased since only a small area is assessed and taken as representative. Small ROIs can also be easily placed incorrectly due to anatomic variations, thereby missing important hemodynamic and metabolic pathophysiology. Yet, significant changes may also be overlooked when image analysis is performed using large a ROI, or if several smaller ROIs are grouped together into a larger cluster representing a single region (e.g., arterial blood supply or border zone). This may produce an "averaging out" effect which can de-emphasize the significance of focal abnormalities.

ROI Versus Visual Analysis

We assessed hemodynamic and metabolic parameters in patients with hemodynamically significant unilateral carotid stenosis using standard ROI and visual analyses. Results obtained by ROI analysis were compared to those obtained from extensive visual evaluation. ROI analysis showed mean values suggestive of early signs of insufficient blood flow ipsilateral to stenosis. These values, however, were not statistically significant when compared to the contralateral homotopic reference regions. This lack of significance goes along with the findings of previous studies which failed to show a correlation between hemodynamics and the degree of stenosis (*6–10*). It may be due to the variance of measured values which is caused by the measurement itself and/or individually different pathophysiology. The use of the contralateral hemisphere in this study as a reference may have led to a conservative estimate of significance, since the contralateral hemisphere might have also been affected by hemodynamic changes.

Visual evaluation, however, demonstrated focal changes suggestive of compromised perfusion and a subsequent effect on tissue metabolism in each patient. These changes occurred exclusively in the ACA and MCA territories and did not appear to involve areas representing borderzones. Furthermore, these changes were often found in the subcortical white matter.

CONCLUSION

The results of our study support the earlier reports of Powers et al. (*7*) and Carpenter et al. (*11*), which found that the presence of hemodynamically significant stenosis did not dictate a pattern of characteristic regional hemodynamic compromise. Our study, however, did demonstrate focal changes in important hemodynamic or metabolic parameters in patients

with hemodynamically relevant carotid artery stenosis (>70%). These effects, however, can be overlooked easily when using standard ROI analysis that is not individually tailored. This limitation becomes increasingly important as PET emerges as a clinical tool and clinicians search for easy methods to interpret PET studies for use in the clinical management of patients. In patients with carotid artery disease, physicians cannot afford to rely on computer-generated analysis programs alone but will also be required to visually assess studies on a case-by-case basis, since those patients who only demonstrate a visually detectable area of decreased perfusion and corresponding elevated oxygen and/or glucose extraction fraction ipsilateral to the carotid stenosis may still benefit from surgical intervention. Therefore, multiparametric PET assessment of the hemodynamic and metabolic status in patients with carotid stenosis should always include both careful visual and standard ROI analysis.

REFERENCES

1. Thompson JE, Patman RD, Talkington CM. Asymptomatic carotid bruit: long-term outcome of patients having endarterectomy compared with unoperated controls. *Ann Surg* 1978;188:308–316.
2. Humphries AW, Young JR, Santilli PH, Beven EG, de Wolfe VG. Unoperated, asymptomatic significant internal carotid stenosis: a review of 182 instances. *Surgery* 1976;80:695–698.
3. Chambers BR, Norris JW. Outcome in patients with asymptomatic neck bruits. *N Engl J Med* 1986;315:860–865.
4. Quinones-Baldrich WJ, Moore WS. Asymptomatic carotid stenosis: rationale for management. *Arch Neurol* 1985;42:378–382.
5. Gibbs JM, Wise RJS, Leenders KL, Jones T. Evaluation of cerebral perfusion reserve in patients with carotid artery occlusion. *Lancet* 1984;I:310–314.
6. Levine RL, Lagreze HL, Dobkin JA, et al. Cerebral vasocapacitance and TIAs. *Neurology* 1989;39:25–29.
7. Powers WJ, Press GW, Grubb RL Jr, Gado M, Raichle ME. The effect of hemodynamically significant carotid artery disease on the hemodynamic status of the cerebral circulation. *Ann Intern Med* 1987;106:27–35.
8. Powers WJ, Grubb RL Jr, Raichle ME. Clinical results of extracranial-intracranial bypass surgery in patients with hemodynamic cerebrovascular disease. *J Neurosurg* 1989;70:61–67.
9. Powers WJ, Tempel LW, Grubb RL. Influence of cerebral hemodynamics on stroke risk: one-year follow-up of 30 medically treated patients. *Ann Neurol* 1989;25:325–330.
10. Powers WJ. Cerebral hemodynamics in ischemic cerebrovascular disease. *Ann Neurol* 1991;29:231–240.
11. Carpenter DA, Grubb RL Jr, Powers WJ. Border zone hemodynamics in cerebrovascular disease. *Neurology* 1990;40:1587–1592.
12. Leblanc R, Yamamoto YL, Tyler JL, Diksic M, Hakim A. Borderzone ischemia. *Ann Neurol* 1987;22:707–713.
13. Leblanc R, Yamamoto YL, Tyler JL, Hakim A. Hemodynamic and metabolic effects of extracranial carotid disease. *Can J Neurol Sci* 1989;16:51–57.
14. Herholz K, Pietrzyk U, Wienhard K, et al. Regional cerebral blood flow measurement with intravenous ^{15}O-water bolus and ^{18}F-fluoromethane inhalation. *Stroke* 1989;20:1174–1181.
15. Herscovitch P, Markham J, Raichle ME: Brain blood flow measured with intravenous $H_2{}^{15}O$. I. Theory and error analysis. *J Nucl Med* 1983;24:782–729.
16. Mintun MA, Raichle ME, Martin WRW, Herscovitch P. Brain oxygen utilization measured with ^{15}O radiotracers and PET. *J Nucl Med* 1984;25:177–187.
17. Grubb RL, Raichle ME, Higgins CS, Eichling JO. Measurement of regional cerebral blood volume by emission tomography. *Ann Neurol* 1978;4:322–328.
18. Reivich M, Kuhl D, Wolf A, et al. The ^{18}F-fluorodeoxyglucose method for the measurement of local cerebral glucose utilization in man. *Circ Res* 1979;44:127–137.
19. Wienhard K, Pawlik G, Herholz K, Wagner R, Heiss W-D. Estimation of local cerebral utilization by positron emission tomography of ^{18}F-2-fluoro-2-deoxy-D-glucose: a critical appraisal of optimization procedures. *J Cereb Blood Flow Metab* 1985;5:115–125.
20. Heiss W-D, Pawlik G, Herholz K, Göldner H, Wienhard K. Regional kinetic constants and cerebral metabolic rate for glucose in normal human volunteers determined by dynamic PET of ^{18}F-2-fluoro-2-deoxy-D-glucose. *J Cereb Blood Flow Metab* 1984;4:212–223.
21. Heiss W-D, Huber M, Fink GR, et al. Progressive derangement of periinfarct viable tissue in ischemic stroke. *J Cereb Blood Flow Metab* 1992;12:193–203.
22. Pietrzyk U, Herholz K, Fink G, et al. Validation of a multi-purpose three-dimensional image registration program. *J Nucl Med* 1994;35:2011–2018.
23. Herholz K, Pawlik G, Wienhard K, Heiss WD. Computer assisted mapping in quantitative analysis of cerebral positron emission tomograms. *J Comput Assist Tomogr* 1985;9:154–161.
24. Damasio H. In: Wood J, ed. *Cerebral blood flow: physiologic and clinical aspects*. New York: McGraw-Hill; 1987:324–332.
25. Vander Eecken HM, Adams RD. Anatomy and functional significance of meningeal anastomoses of human brain. *J Neuropathol Exp Neurol* 1953;12:132–157.
26. Archie JP Jr, Feldtman RW. Critical stenosis of the internal carotid artery. *Surgery* 1981;89:67–70.
27. De Weese JA, May AG, Lipchik EO, Rob CG. Anatomic and hemodynamic correlations in carotid artery stenosis. *Stroke* 1970;1:149–157.
28. Boysen G, Ladegaard-Pedersen HJ, Valentin N, Engell HC. Cerebral blood flow and internal carotid artery flow during carotid surgery. *Stroke* 1970;1:253–260.
29. Huber M, Hojer C, Neveling M, Fink GR, Herholz K. Transcranial doppler and ^{15}O-water PET findings in patients with acute brain infarction and middle cerebral artery stenosis. *J Stroke Cerebrovasc Dis* 1994;4:23–29.
30. Friston KJ, Frith CD, Liddle PF, Frackowiak RSJ. Comparing functional PET images: the assessment of significant change. *J Cereb Blood Flow Metab* 1991;11:690–699.

Modeling of Fluorine-18-6-Fluoro-L-Dopa in Humans

Lindi Wahl and Claude Nahmias

Department of Nuclear Medicine, McMaster University Medical Centre Hamilton, Ontario, Canada

Fluorine-18-6-fluoro-L-Dopa (F-Dopa) has been used successfully to evaluate striatal dopaminergic function in humans. The kinetic analysis of F-Dopa studies, however, is confounded by the presence of [^{18}F]6-fluoro-3-O-methyl-L-Dopa (OMFD), the major metabolite of F-Dopa formed in the periphery that crosses the blood-brain barrier. We present results of compartmental analysis in subjects in whom we independently measured the kinetics of OMFD in the blood and striatum, and used this knowledge to solve for the kinetics of F-Dopa. **Methods:** The kinetics of F-Dopa in striatum were measured with PET from 0 to 150 min after an intravenous bolus injection of tracer in four normal subjects and two patients suffering from Parkinson's disease. On a separate occasion, the kinetics of OMFD were determined in the plasma and striatum of the same individuals. The measured OMFD kinetics of each individual allowed us to reduce the number of compartments and rate constants which have to be solved for any compartmental analysis of the kinetics of F-Dopa. **Results:** A two-compartmental, three rate-constant model was sufficient to describe the time course of F-Dopa and its metabolites in the striatum. The rate constant (k_{21}) representing the decarboxylation rate of F-Dopa was 0.0124 min^{-1} in the normal subjects, and 0.0043 min^{-1} in the parkinsonian patients. **Conclusion:** The data do not support the need to include a fourth rate constant representing the egress of F-Dopamine and its metabolites. The forward transport rates for F-Dopa and OMFD from plasma to striatum are very similar in humans.

Key Words: fluorine-18-F-Dopa; compartmental analysis; PET; dopamine metabolism; fluorine-18-OMFD

J Nucl Med 1996; 37:432–437

Dopamine is a neurotransmitter in the central nervous system found predominantly in the nigrostriatal neurons. Disturbances in dopamine metabolism are a key feature in neuro-degenera-

Received Jan. 4, 1995; revision accepted Jul. 5, 1995

For correspondence or reprints contact: Claude Nahmias, PhD, Department of Nuclear Medicine, McMaster University Medical Centre, 1200 Main St. West, Hamilton, Ontario, Canada, L8N 3Z5.